Bull. Mater. Sci. (2019) 42:183
https://doi.org/10.1007/s12034-019-1874-5

First principles investigation of the structural, electronic, thermal and transport properties of new ternary auride X_3AuO (X = K and Rb) semiconductors

O YOUB*, Z AZIZ, B BOUABDELLAH, D CHENINE and T LANTRI
Laboratory of Technology and Solid Properties, BP227 Abdelhamid Ibn Badis University, 27000 Mostaganem, Algeria
*Author for correspondence (oumelkheiryoub@yahoo.com)

MS received 29 November 2018; accepted 20 February 2019; published online 3 June 2019

Abstract. We report the structural, electronic, thermal and transport properties of two new ternary aurides containing gold atom X_3AuO (X = K and Rb) using the full-potential linearized augmented plane wave method, based on the density functional theory. To describe the exchange-correlation potential, we have employed the generalized gradient approximation–Perdew–Burke–Ernzerhof (GGA–PBE) scheme of the GGA. The computed ground state properties are in good accordance with the experiments. Moreover, Tran–Blaha-modified Becke–Johnson (TB–mBJ) potential improves the electronic properties and gives accurate band gaps. Both anti-perovskites X_3AuO are semiconductors with an indirect band gap. Furthermore, the inclusion of spin–orbit coupling effects on the band structure along with TB–mBJ approximation splits the valence band of our compounds and reduces their band gap energy. The thermodynamic properties including heat capacity (C_V), thermal expansion (α) and Debye temperature (Θ_D) are also estimated. The transport properties as function of temperature are calculated using the BoltzTrap code; therefore, these two materials are very appropriate for thermoelectric devices at high temperatures.

Keywords. DFT; electronic properties; spin–orbit coupling effect; GGA; first-principles calculations; thermal properties.

1. Introduction

Cubic inverse perovskites have immense technological interest considering their application in giant magneto resistance [1–5] and nearly zero temperature coefficient of resistance [6]. These compounds pose a wide range of properties, such as superconducting, magnetic, semiconducting and metallic properties [7–11]. Thus, it is very indispensable to search new inverse perovskites with significant physical properties which are appropriate in modern semiconductor technology.

Recently, the existence of anionic gold (Au^{-1}) in some alloys has attracted attention due to its electron affinity, which is very similar to iodine [12]. The study of anionic gold (Au^{-1}) chemistry is of great importance because of its excellent properties, which are ranging from metallic for KAu to semiconducting for RbAu and CsAu with CsAu having a band gap of ≈2.6 eV [13–15]. Moreover, materials contain gold involved significant attention from the adjustment of the Schottky contact height at Au contacts with semiconductors [16] to the development of field-emission properties [17]. The presence of Au-anions is also potentially important in catalytic processes [18,19]. Several compounds containing anionic gold (Au^{-1}) have also been reported, such as A_3AuO (A = K, Rb and Cs) [20,21] and Ba_8As_5Au [22]. To attain a deeper and clear knowledge about the chemistry of auride and its bonding characters, Feldmann and Jansen [21] use an X-ray structure to synthesize novel Rb_3AuO and K_3AuO. The novel ternary oxides K_3AuO and Rb_3AuO contain auride anions according to the ionic description $(M^+)_3Au^{-1}0^{2-}$ (M = K and Rb). An appropriate method for this purpose is X-ray absorption spectroscopy. In particular, the X-ray absorption near edge structure efficiently indicates the presence of auride anions in K_3AuO and Rb_3AuO [23,24]. Using this method, they found that K_3AuO and Rb_3Au0 crystallize in the ideal cubic anti-perovskite structure type (anti-$CaTiO_3$). Gold adopts the Ca-position, oxygen adopts the Ti-position with a = 5.240 Å for K_3AuO and a = 5.501 Å for Rb_3AuO [25]. The purpose of this work is to use *ab-initio* calculations to study the structural, electronic, thermodynamic and thermoelectric properties of two novel ternary oxides containing anionic gold atom X_3AuO (X = K and Rb) using the full-potential linearized augmented plane wave (FP-LAPW) method within generalized gradient approximation–Perdew–Burke–Ernzerhof (GGA–PBE) and Tran–Blaha-modified Becke–Johnson (TB–mBJ) (with and without spin–orbit coupling (SOC)) approaches.

2. Method of calculations

In this paper, we investigated the structural, electronic, thermodynamic and thermoelectric properties using the

FP-LAPW method within the frame work of the density functional theory [26–28], implemented in the WIEN2K code [29]. The experimental lattice constants are 5.240 and 5.501 Å for K_3AuO and Rb_3AuO, respectively [25,30]. Furthermore, for the exchange-correlation functional, we have used the GGA functional developed by PBE [31]. The TB–mBJ potential [32–36] was employed to achieve the most accurate band gaps. We have also performed a calculation including the spin–orbit effect on the band structure along with the TB–mBJ approximation. The considered ternary oxides X_3AuO (X = K and Rb) were studied in an ideal cubic anti-perovskite structure (space group *Pm*-3*m*). We have employed a mesh of 1000 k-points in the whole Brillouin zone to perform self-consistent field calculations. The energy separation between the core and valence states is maintained at −6.0 Ry. To achieve energy and charge convergence, the $R_{MT} * K_{Max}$ is equal to 7.0, where R_{MT} is the smallest muffin-tin (MT) radius and K_{Max} is the maximum value of the wave vector. The MT radii are taken as 2.50 Ry for Au, 1.8 Ry for O, 1.95 Ry for K and 2.29 Ry for Rb.

3. Results and discussion

3.1 *Structural properties*

To determine the structural parameters of the studied compounds, we have employed the GGA–PBE approach. The new ternary oxides X_3AuO (X = K and Rb) crystallize as anti-perovskites with cubic symmetry (space group *Pm*-3*m*). The calculated ground states including lattice parameters (a_0), bulk modulus (B_0) and its pressure derivative (B_p) at zero pressure are given in table 1 together with the experimental results for comparison [25,30,37]. The total energies for different volumes are calculated and fitted to the Birch–Murnaghan's equation of state around the experimental unit-cell volume [38,39]. The obtained lattice parameters are a_0 = 5.242 Å for K_3AuO and a_0 = 5.512 Å for Rb_3AuO, which are in excellent agreement with the experimental results [25,30]; a_0 = 5.240 and 5.501 Å for K_3AuO and Rb_3AuO, respectively. From table 1, one can observe that the lattice constant a_0 increases in the sequence as a_0 (Rb_3AuO) > a_0 (K_3AuO). Considering that the lattice constant increases with an increase in the atomic radius of alkali-metal (R_{Rb} = 1.72 Å > R_K = 1.64 Å) [40]. When comparing the obtained results of the volume within GGA–PBE, the computed results deviate from the measured one within 0.09% for K_3AuO and 0.50% for Rb_3AuO [25,37]. No experimental or theoretical results for the bulk modulus (B_0) and its pressure derivative (B_P) are available in the literature for the X_3AuO compounds to be compared with the present calculations.

Table 1. Calculated structural equilibrium lattice constant a_0, bulk modulus B_0, its pressure derivatives B_P and the volume of the cubic K_3AuO and Rb_3AuO using the GGA–PBE calculations in comparison with available experimental works.

Parameter	Method	K_3AuO	Rb_3AuO
a_0 (Å)	GGA–PBE	5.242	5.512
	Exp.	5.240[a]	5.5010[a,b]
B_0 (GPa)	GGA–PBE	18.4472	15.4590
	Exp.	—	—
B_p (GPa)	GGA–PBE	4.5583	4.8072
	Exp.	—	—
V (Å^3)	GGA–PBE	144.04	167.46
	Exp.	143.9[a]	166.55[c], 166.4[a]

[a]Ref. [25], [b]ref. [30], and [c]ref. [37].

3.2 *Electronic properties*

As the TB–mBJ seems to determine the most accurate band gap compared to the GGA–PBE, we used it to perform the calculations of the electronic structure of K_3AuO and Rb_3AuO at the obtained equilibrium lattice parameters. Figure 1 displays the calculated band structures for both compounds along high symmetry directions in the Brillouin zone using GGA–PBE and TB–mBJ approaches (without SOC). From figure 1a, b, d and e, we observed that the valence band maximum (VBM) occurs at the Γ-point, while the conduction band minimum (CBM) is situated at the X-point, therefore, K_3AuO and Rb_3AuO indicate an indirect band gap (Γ–X) values of 0.47 and 0.14 eV from GGA–PBE and 1.72 and 1.34 eV when using TB–mBJ, respectively. As is known, the presence of a heavy element in materials in the medium range of atomic numbers (up to about 54) [41] requires the use of the SOC effect. Then, we have calculated the band structure by including SOC effects along with the TB–mBJ approach and the results are presented in figure 1c and f. The inclusion of the SOC effect splits the valence band of the two materials. Therefore, the band gap energy between the CBM and VBM is reduced. To gain a deeper insight into the electronic band structure, the total and partial densities of states are computed and depicted in figure 2 using GGA–PBE and TB–mBJ approximations. The general features of the densities of states have similarity for both compounds, except for the band gap values and positions of the peaks. Applying the GGA–PBE method, we observe that the valence band of both studied compounds can be divided into two groups as shown in figure 2a–c. The top of the valence band is dominated by O-p states with weak hybridization with K-p (Rb-p) states. The second region is essentially dominated by Au-s and Au-d states. Whereas, when using the TB–mBJ approach, the valence band consists of three parts as shown in figure 2b–d. The first peak is composed predominantly of Au-d states, while the next peak corresponds to Au-s states and the topmost of the UVB states is mainly due to O-p orbitals. Moreover, the top of the conduction band is formed by Au-p states and the bottom band is essentially due to the unoccupied K-d (Rb-d) orbitals with a small contribution of Au-p for two compounds using both methods.

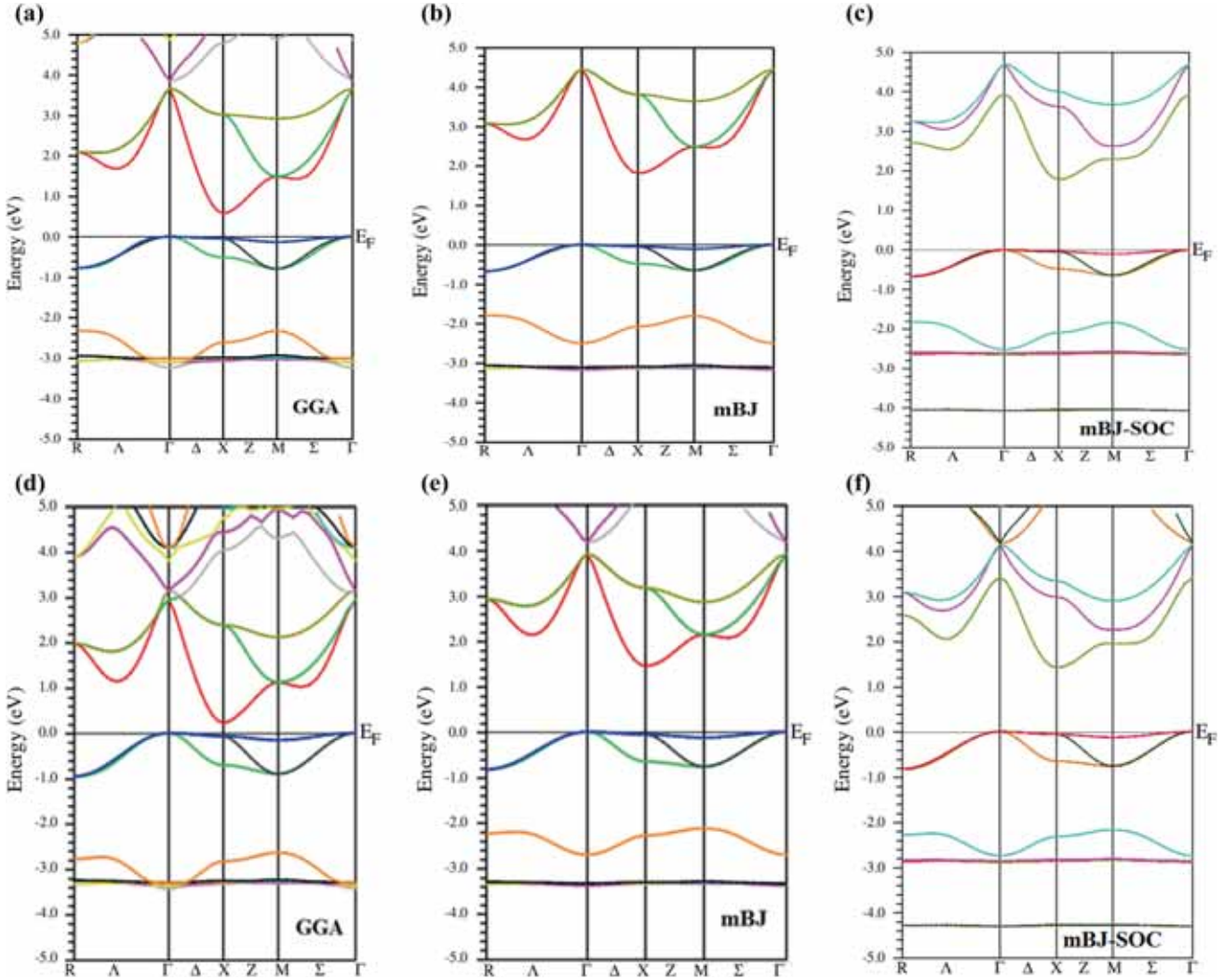

Figure 1. Calculated band structures for (**a–c**) K_3AuO and (**d–f**) Rb_3AuO at equilibrium lattice constants, using GGA–PBE and TB–mBJ approaches (with and without SOC effect). The Fermi level is located at (E_F = 0.0 eV).

3.3 *Thermodynamic properties*

Thermodynamic properties are being very crucial in explaining some characteristics of semiconductors and semiconductor devices, especially at higher temperatures and pressures. The quasi-harmonic Debye model as implemented in the Gibbs program [42] is applied to calculate the volume V, heat capacity at constant volume C_V, thermal expansion α and Debye temperature Θ_D. The calculated results are obtained at temperature ranging from 0 K to a temperature below the melting point (T_m), 799 and 850 K for K_3AuO and Rb_3AuO, respectively [43] and pressure from 0 to 20 GPa. Our results are shown in figure 3. Temperature dependences of the volume for K_3AuO and Rb_3AuO are displayed in figure 3a. It can be seen that both compounds have nearly similar characters with a small difference in volumes. We observe a very moderate increase in the volume with an increase in temperature for $T < 100$, however, for $T > 100$, the volume remains constant for different pressures. At room temperature and zero pressure, the calculated equilibrium primitive cell volume is 159.57 and 187.66 Å^3 for K_3AuO and Rb_3AuO, respectively. Heat capacity C_V *vs.* temperature for X_3AuO (X = K and Rb) are shown in figure 3b. For both anti-perovskite materials, heat capacity reveals similar features. From figure 3b, we can see that at low temperature ($T < 300$), C_V increases rapidly, which is proportional to T^3 [44]. Whereas, a tardily increase at high temperature reaching to the petit Dulong limit [45], which is common to all solids at high temperatures. Moreover, the tendency of matter to change its size with a changing temperature is described by another important thermodynamic parameter, i.e., the thermal expansion (α). The parameter α as a function of temperature for both compounds is presented in figure 3c. α increases rapidly with T at low temperature and converges to a constant

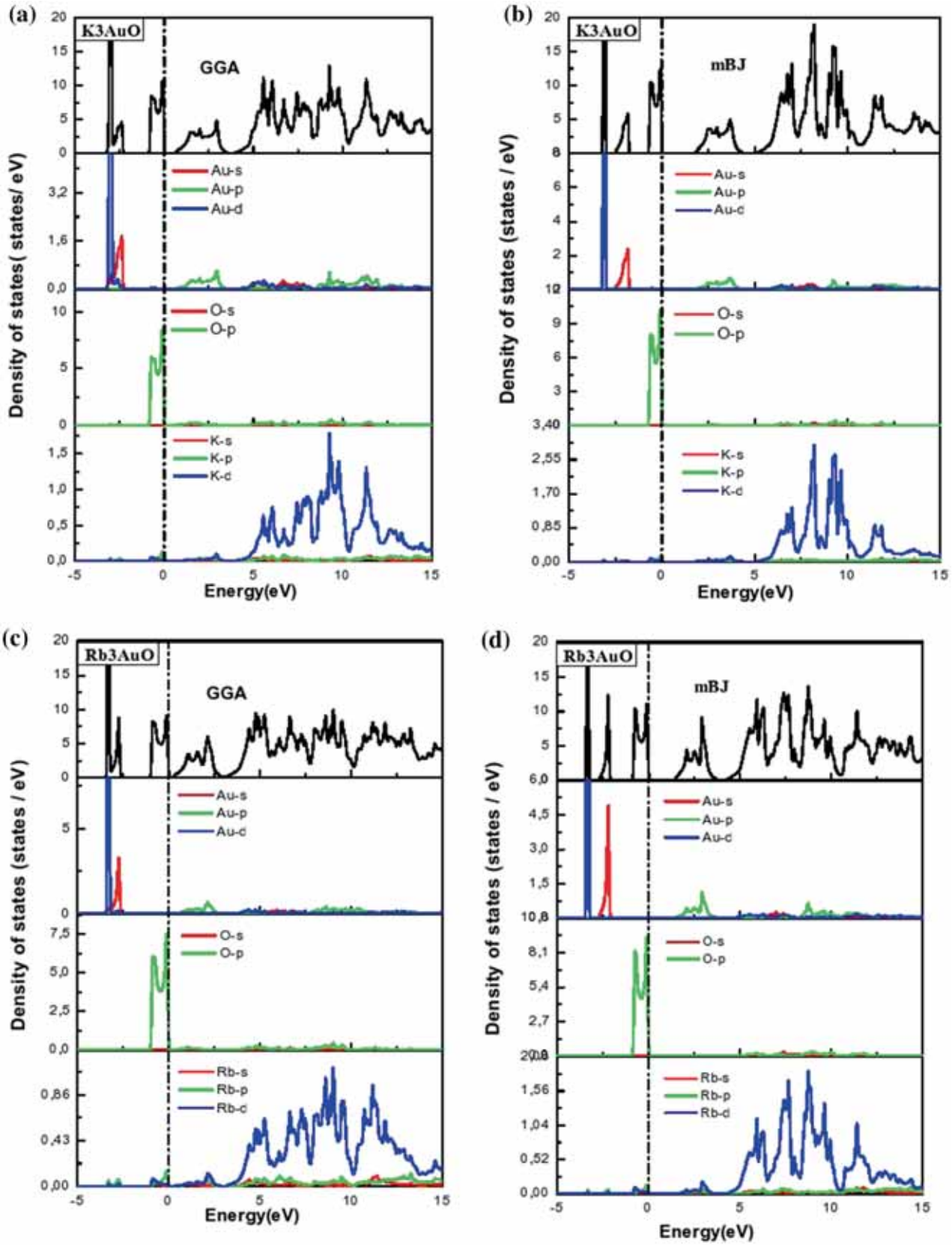

Figure 2. Total and partial densities of states of the cubic anti-perovskites (**a** and **b**) K_3AuO and (**c** and **d**) Rb_3AuO using GGA–PBE and TB–mBJ approximations. The Fermi level is set to 0 eV.

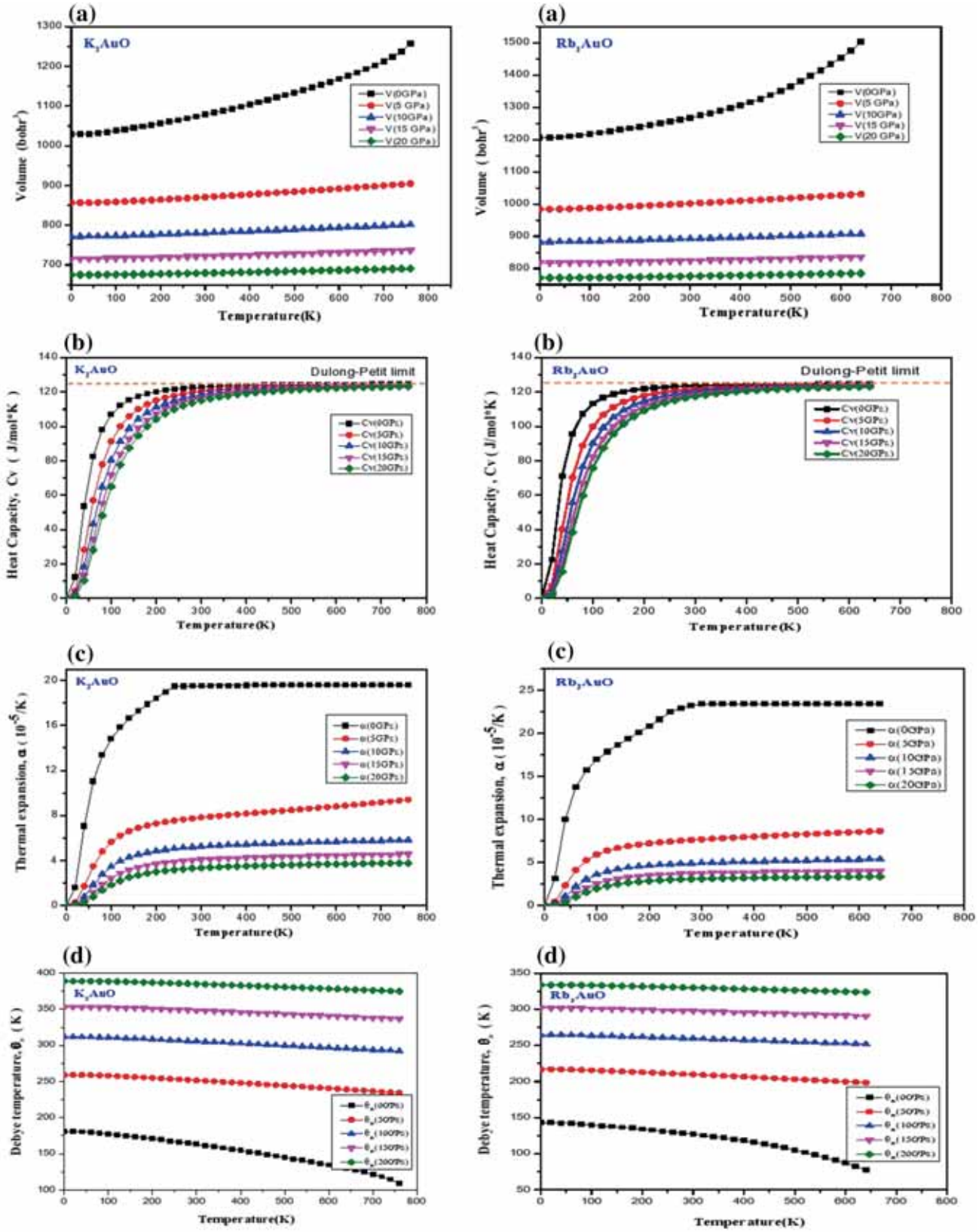

Figure 3. Temperature dependence of (**a**) the volume V (**b**) the specific heat at constant volume C_V, (**c**) the thermal expansion coefficient α and (**d**) the Debye temperature Θ_D of K_3AuO and Rb_3AuO anti-perovskites.

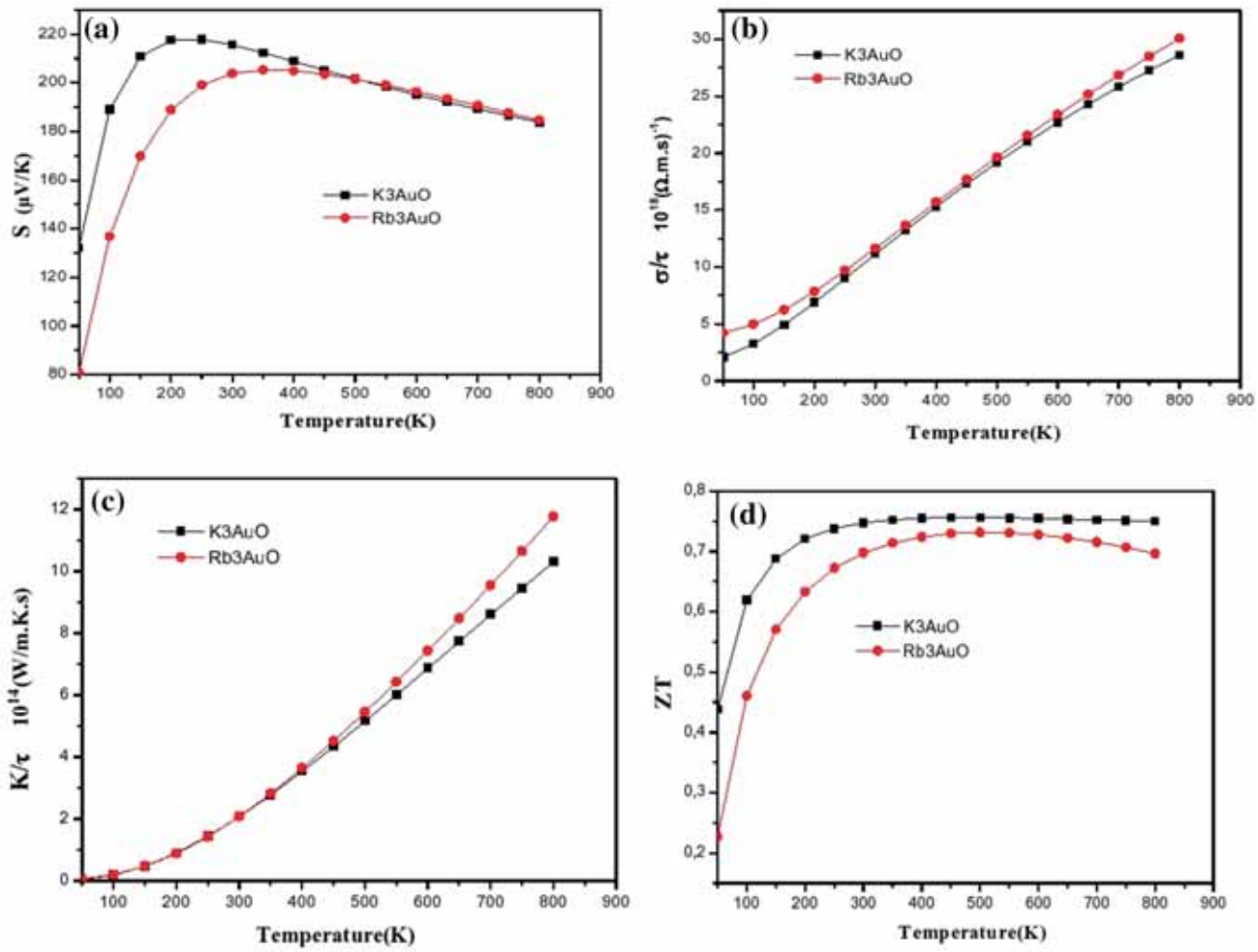

Figure 4. (**a**) Seebeck coefficient S, (**b**) electrical conductivity σ, (**c**) thermal conductivity K and (**d**) figure of merit ZT as functions of temperature for the two compounds of K_3AuO and Rb_3AuO.

value at high temperatures. The Debye temperature is a fundamental parameter that provides us valuable information about diverse physical properties including elastic constants, specific heat and melting temperature. The Debye temperature is the highest temperature that can be achieved due to a single normal vibration. The Debye temperature is given by [46]:

$$\Theta = \frac{\hbar}{K}\left[6\pi^2 V^{1/2} n\right]^{1/3} f(\sigma)\sqrt{\frac{B_s}{M}}, \tag{1}$$

where M is the molecular mass per unit cell and B_s is the adiabatic bulk modulus, which is given by the following equation [47]:

$$B_s \cong B(V) = V\left(\frac{d^2E(V)}{dV^2}\right). \tag{2}$$

From figure 3d, we can see the variations of the Debye temperature *vs.* temperature for K_3AuO and Rb_3AuO. It can be seen that the Debye temperature of two compounds decreases slightly and linearly as the temperature increases. From equations (1 and 2), we conclude that the Debye temperature depends only on the volume of the unit cell. Moreover, it is clear that for constant temperature, the Debye temperature of X_3AuO increases almost linearly with the decrease in the volume, (figure 3a).

3.4 *Thermoelectric properties*

Over the past decade, researchers are involved in finding more efficient materials for electronic refrigeration and power generation [48]. Thermoelectric materials become more important as alternative energy sources. A thermoelectric material is a material that can be used to convert thermal energy into electric energy or provide refrigeration directly from electric energy. The thermoelectric efficiency of a material is quantified by a figure of merit ($ZT = \sigma S^2 T/\kappa$) [49–51], which contains three physical quantities; Seebeck coefficient (S), electrical conductivity (σ) and thermal

conductivity (k). The Seebeck coefficient tells us how many volts per degree temperature difference are generated. The electrical conductivity determines how well a material conducts electricity, and the thermal conductivity is a measure of how well heat is conducted. The calculated Seebeck coefficient (S), electrical conductivity (σ), thermal conductivity (k) and figure of merit (ZT), which are computed by the equations reported in refs [52,53] and represented in figure 4a–c for two compounds K_3AuO and Rb_3AuO. Moreover, the BoltzTrap code [54] as implemented in the Wien2k code is applied to study the transport properties of K_3AuO and Rb_3AuO materials. To ensure the convergence of our transport properties, a dense k-mesh is used. In the present case, thermoelectric properties are computed within a temperature range of 50–900 K. Figure 4a shows the plots of the Seebeck coefficient (thermo-power) for K_3AuO and Rb_3AuO. The positive value of the Seebeck coefficient confirms the p-type nature of these materials. It can be seen that the Seebeck coefficient increases rapidly with temperature and reaches its maximum value 217.51 $\mu V\,K^{-1}$ (205.31 $\mu V\,K^{-1}$) at 250 K (350 K) for K_3AuO (Rb_3AuO), and thereafter, decreases to attain a value of 183.54 $\mu V\,K^{-1}$ at 800 K for both compounds. The value of the Seebeck coefficient at room temperature is 215.68 and 203.83 $\mu V\,K^{-1}$ for K_3AuO and Rb_3AuO, respectively. Therefore, the studied semiconductors exhibit good thermoelectric features. Figure 4b represents the electrical conductivities of K_3AuO and Rb_3AuO. The electrical conductivity increases linearly with temperature, besides at given temperature, the electrical conductivity is approximately the same for two anti-perovskites. At 800 K, K_3AuO and Rb_3AuO record a maximum value of electrical conductivity as 28.61×10^{18} and 30.07×10^{18} $(\Omega ms)^{-1}$, respectively, which means that K_3AuO and Rb_3AuO compounds have excellent electrical conductivities.

In semiconductor materials, heat is transferred mostly because of lattice vibrations, whereas in metals, free electrons are the good source of thermal conductivity [55,56]. The calculated thermal conductivities are displayed in figure 4c. From this figure, we show that thermal conductivity of the examined compounds remains nearly the same until 400 K and then increases gradually with an increase in temperature to achieve the maximum value of 11.78×10^{14} W mK^{-1}s^{-1} (10.31×10^{14} W mK^{-1}s^{-1}) at 800 K due to the electronic vibrations. To examine the performance of our studied materials, we have also calculated another important parameter; the dimensionless figure of merit (ZT) for K_3AuO and Rb_3 AuO and represented in figure 4d. We observe that ZT of K_3AuO (Rb_3AuO) increases rapidly with an increase in temperature to reach its maximum value of 0.75 (0.73) at 500 K, and remains constant with an increase in temperature, which indicates that K_3AuO is the best thermoelectric material. Thus, the considered anti-perovskites X_3AuO (X = K and Rb) indicate very promising materials for thermoelectric applications in a high-temperature range.

4. Conclusion

In summary, we systematically investigated the structural, electronic, thermal and transport properties of new ternary aurides containing gold atom X_3AuO (X = K and Rb) for the first time by means of the FP-LAPW method. The study reveals that the anti-perovskites X_3AuO crystallize in cubic symmetry (space group Pm-3m) and their structural parameters are in good agreement with the experimental data. The GGA–PBE and TB–mBJ approaches show that both anti-perovskites are indirect band gap semiconductors. Furthermore, the inclusion of SOC in the TB–mBJ approach splits the valence band of X_3AuO compounds and reduces their band gaps. The thermal properties are also computed using the quasi-harmonic Debye model and found that the heat capacity (C_V) is close to the Dulong–Petit limit. Furthermore, the effects of temperature on thermoelectric parameters are investigated using the BoltzTraP code, and the positive Seebeck coefficient confirms that K_3AuO and Rb_3AuO are p-type semiconductors. These two materials are expected to have significant applications in thermoelectric and thermoelectric devices at high temperatures.

References

[1] Kim W S, Chi E O, Kim J C, Choi H S and Hur N H 2001 *Solid State Commun.* **119** 507
[2] Wang B S, Tong P, Sun Y P, Luo X, Zhu X B, Li G *et al* 2009 *Europhys. Lett.* **85** 47004
[3] Joshi D A, Kumar N, Thamizhavel A and Dhar S K 2009 *Phys. Rev. B* **80** 224404
[4] Pandey A, Mazumdar C and Ranganathan R 2009 *Appl. Phys. Lett.* **94** 172509
[5] Wen Y, Wang C, Sun Y, Nie M, Fang L and Tian Y 2009 *Solid State Commun.* **149** 1519
[6] Chi E O, Kim W S and Hur N H 2001 *Solid State Commun.* **120** 307
[7] Vaitheeswaran G, Kanchana V, Svane A and Delin A 2007 *J. Phys.: Condens. Matter* **19** 326214
[8] Ram S and Kanchana V 2014 *Solid State Commun.* **181** 54
[9] Ramanna J, Yedukondalu N, Ramesh Babu K and Vaitheeswaran G 2013 *Solid State Sci.* **20** 120
[10] Kanchana V and Ram S 2012 *Intermetallics* **23** 39
[11] Kanchana V 2009 *EPL J.* **87** 26006
[12] Hotop H and Lineberger W C 1975 *J. Phys. Chem. Ref.* **4** 539
[13] Spicer W, Sommer A and White J 1959 *Phys. Rev.* **115** 57
[14] Liu T 1975 *Phys. Rev. B* **12** 3008
[15] Wooten F and Condas G 1963 *Phys. Rev.* **131** 657
[16] Wertheim G, Rowe J, Chiang C, Malic R and Buchanan D 1995 *Surf. Sci.* **330** 27
[17] Bernatskii D P and Pavlov V G 2006 *Tech. Phys. Lett.* **32** 579
[18] Vansanten R and Kuipers H 1987 *Adv. Catal.* **35** 265
[19] Zomerdijk J and Hall M 1981 *Cat. Rev. Sci. Eng.* **23** 163
[20] Feldmann C and Jansen M 1993 *Angew. Chem. Int. Ed. Engl.* **32** 1049
[21] Feldmann C and Jansen M Z 1995 *Z. Anorg. Allg. Chem.* **621** 201

[22] Nuss J and Jansen M Z 2002 *Z. Kristallogr. NCS* **217** 313
[23] Koningsberger D C and Prins R 1988 *X-ray absorption: techniques of EXAFS, SEXAFS and XANES* (New York: Wiley)
[24] Aganval B K 1979 *X-ray spectroscopy* (Berlin: Springer)
[25] Kienast G, Verma L and Klemm K 1961 *Z. Anorg. Allg. Chem.* **310** 143
[26] Hohenberg P and Kohn W 1964 *Phys. Rev. B* **136** 864
[27] Kohn W and Sham L J 1965 *Phys. Rev.* **140** 1133
[28] Slater J C 1972 *Adv. Quant. Chem.* **6** 1
[29] Blaha P, Schwarz K, Madsen G K H, Kvasnicka D and Luitz J 2001 *WIEN2 K, An augmented plane wave plus local orbitals program for calculating crystal properties, Karlheinz Schwarz* (Wien, Austria: Technische Universitat)
[30] Wertheim G K, Cohen R L, Crecelius G, West K W and Wernick J H 1979 *Phys. Rev. B* **20** 860
[31] Perdew J P, Burke K and Ernzerhof M 1996 *Phys. Rev. Lett.* **77** 3865
[32] Perdew J P and Wang Y 1986 *Phys. Rev. B* **33** 8822
[33] Perdew J P 1991 *Electronic structure of solids* (Berlin: Academie Verlag) p 11
[34] Perdew J P and Burke K 1996 *Int. J. Quantum Chem.* **57** 309
[35] Azahaf C, Zaari H, Abbassi A, Ez-Zahraouy H and Benyoussef A 2015 *Opt. Quant. Electron.* **47** 2889
[36] Marezio M, Remeika J P and Dernier P D 2008 *Acta Cryst. B* **26** 1970
[37] Holleman A F and Wiberg E 1960 *Lehrbuch der anorganischen Chemie, Walter de Gruyter & Co*. **703** 47
[38] Birch F 1947 *Phys. Rev.* **71** 809
[39] Murnaghan F D 1944 *Proc. Natl. Acad. Sci. USA* **30** 91
[40] Moreira R L and Dias A 2007 *J. Phys. Chem. Solids* **68** 1617
[41] Karlheinz S, Peter B and Trickey S B 2010 *Mol. Phys.* **108** 3147
[42] Blanco M A, Francisco E and Luana V 2004 *Comput. Phys. Commun.* **158** 57
[43] Martin J 2008 *Chem. Soc. Rev.* **37** 1826
[44] Debye P 1912 *Ann. Phys.* **39** 789
[45] Petit A T and Dulong P L 1819 *Ann. Chim. Phys.* **10** 395
[46] Blonco M A, Pendas A M, Francisco E, Recio J M and Franco R 1996 *J. Mol. Struct. Theochem.* **368** 245
[47] Blonco M A, Francisco E and Luana V 2004 *Comput. Phys. Commun.* **158** 57
[48] Tritt T M 2000 *Recent trends in thermoelectric materials research semiconductors and semimetals* R K Willardson and E Weber (eds) (New York: Academic Press) vols 69–71
[49] Yousuf S and Gupta D C 2017 *Indian J. Phys.* **91** 33
[50] Bhat T M and Gupta D C 2016 *RSC Adv.* **6** 80302
[51] Bhat T M and Gupta D C 2016 *J. Electron Mater.* **45** 6012
[52] Yousuf S and Gupta D C 2017 *Mater. Chem. Phys.* **192** 33
[53] Khandy S A and Gupta D C 2017 *Int. J. Quantum Chem.* **117** e25351
[54] Madsen G K H and Singh D J 2006 *Comput. Phys. Commun.* **175** 67
[55] Nuwayhid R, Rowe D and Min G 2003 *Renew. Energy* **28** 205
[56] Rabina O. Lin Y M and Dresselhaus M S 2001 *Appl. Phys. Lett.* **79** 81